Article

Zonal-Based Optimal Microgrids Identification

Abdullah Albaker *[iD], Mansoor Alturki [iD], Rabeh Abbassi [iD] and Khalid Alqunun

Department of Electrical Engineering, College of Engineering, University of Ha'il, Ha'il 81451, Saudi Arabia; m.alturki@uoh.edu.sa (M.A.); r.abbassi@uoh.edu.sa (R.A.); kh.alqunun@uoh.edu.sa (K.A.)
* Correspondence: af.albaker@uoh.edu.sa

Abstract: Even though many studies have been deployed to determine the optimal planning and operation of microgrids, limited research was discussed to determine the optimal microgrids' geographical boundaries. This paper proposes a zonal-based optimal microgrid identification model aiming at identifying the optimal microgrids topology in the current distribution systems through zoning the network into several clusters. In addition, the proposed model was developed as a mixed-integer linear programming (MILP) problem that identifies the optimal capacity and location of installing distributed energy resources (DERs), including but not limited to renewable energy resources and Battery Energy Storage Systems (BESS), within the determined microgrid's boundaries. Moreover, it investigates the impact of incorporating the BESS in boosting the DERs' penetration on the optimal centralized microgrid. Numerical simulations on the IEEE-33 bus test system demonstrate the features and effectiveness of the proposed model on identifying the optimal microgrid geographical boundaries on current distribution grids as well as its capability on defining the optimal sizes and locations of installing DERs within the microgrid's zonal area.

Keywords: battery energy storage system (BESS); distributed energy resources (DERs); microgrids topology; mixed-integer linear programming; optimization

1. Introduction

Incorporating renewable energy resources into current distribution grids in an intelligent and optimal manner attracts the attention of researchers and intellectuals due to its significance in conserving natural energy resources and its affirmative impact on the environment [1–4]. Renewable energy resources started to become attractive during the mid of 1970s to preserve natural/conventional fuel sources and became even more substantial during the 1980s after diagnosing the enormous impact of traditional power system sources on global warming and environmental pollution [5–7]. Renewable energy resources such as solar photovoltaics, wind turbines, fuel cell, hydropower, ocean energies, biomass, and geothermal deliver sustainable and clean energy to end-user consumers and are considered fundamental resources in energy-saving communities [8–11]. However, it is challenging to integrate into existing distribution grids due to their intermittency and volatility characteristics.

One of the recently emerged technology, microgrids, about two decades ago, is projected to expand the renewable energy resources penetration into the distribution grids with a higher degree of resiliency and reliability [12–16]. The microgrid is a controllable small-scale power system comprised of a mix of Distributed Energy Resources (DERs) that are installed next to predefined loads, i.e., the loads within the microgrid's controllable boundaries, to provide the system with sufficient requirements of reliability and resiliency and to increase the projected economic benefits [17–21]. The microgrid can operate connected to the main power grid and as isolated from the main power grid, i.e., in grid-connected and islanded modes, respectively. In the grid-connected mode, the microgrid has a chance to exchange its local power generation with the main power grid for mutual benefits, as it can support the distribution grid with an instant power generation during peak power

demand, which increases its economic benefits by selling its surplus power generation, and also still has the path to import its further need of power to supply its local load demand [22–25]. On the other hand, the microgrid is shifted to operate in the islanded mode during upstream incidents to protect its equipment from unexpected faulty conditions whilst supplying its local loads demands with sufficient power requirement [26–28]. The microgrid's optimal operation and planning were extensively discussed and studied in the literature [29–32]. However, recognizing the microgrids' actual sizing and boundaries on the current distribution grids has not been sufficiently discussed and investigated.

Dividing the distribution network into multiple clusters or zones reliefs is part of the operational challenges that occur when accommodating large-scale DERs into existing distribution systems. However, it may create further challenges that require updating distribution systems infrastructure. The concept of zoning the power distribution system into multiple zones or clusters was discussed in the literature [33–38]. In [39], a zonal operation scheme of distributed generators was presented in order to regulate the voltage in a distribution network based on SCADA information, where the system is divided into several voltage regulation zones based on the distribution network's impedance data and taking into account high penetration of photovoltaic systems (PVs). The study in [40] presented a dynamic zone division scheme based on the power system sensitivity analysis to divide a large power system into smaller zonal areas, where the proposed study is conducted to build the functional module of the energy management system in the Guangdong power grid. In [41], the authors proposed a decentralized voltage control scheme based on distributed generators that provide voltage support in distribution networks in a short- and long-term manner. The system is divided into several local controllable zones in order to determine the voltage control limits for each distributed generator, whereas the divided controllable zones are determined based on the distributed generators' location, number, and size and are reconfigurable in response to the real-time network topology changes. The study in [42] proposes a coordinated voltage control strategy to control the distribution network voltage regulation considering a high penetration of distributed generators (DGs) in the distribution system, where both DGs and On-Load Tap Changer are considered as voltage regulators for the distribution system. Moreover, it adopts a hierarchical voltage regulation method to eliminate the over-limit voltage in each voltage control zone. In [43], a novel hybrid optimization algorithm based on a combination of modified shuffled frog leaping algorithm (MSFLA) and improved particle swarm optimization (IPSO) was proposed to solve the distribution feeder reconfiguration problem along with the optimal capacitor allocation. The study in [44] proposed a modified honey bee mating optimization algorithm to solve the dynamic distribution feeder reconfiguration problem considering system loss, operational cost, and voltage stability index. In [45], a modified particle swarm optimization algorithm (MPSO) was proposed to solve the dynamic distribution feeder reconfiguration problem for energy management in the distribution system. In [46], a centralized control approach was proposed to optimize the voltage profile of the distribution systems based on identifying the set-points of controllers of the DERs that are coupled to the distribution grid. The distribution network is divided into multiple voltage control zones through the execution of the sensitivity analysis of the system, which is also used to determine the pilot node in each voltage control zone. In [47], a hierarchical clustering-based zone division was proposed to divide the power network into an identified number of smaller zones in order to facilitate the operation and control for system operators. The formation of the zones is accomplished based on the inter- and intra-cluster distances between each node in the system. The study in [48] proposed a hybrid algorithm based on hierarchical evolution for solving large-scale multi-zones power system economic dispatch problems considering complex practical constraints. In [49], a decentralized adaptive emergency control scheme was proposed to regulate the voltage instability issues of the power system by splitting the power system into several zones taking into account the concept of electrical distance during the division process. In [50], a hybrid approach that combines evolutionary and conventional graph partitioning algorithms was proposed to divide the power system net-

work into smaller clusters or zones based on cluster connectedness and sizes, as well as the number of zones and the electrical distances in order to support the control and planning applications. Even though several studies were conducted that utilize dividing the power distribution network into several smaller zones, identifying the optimal microgrids' actual locations and boundaries on the current power distribution systems has not been explicitly investigated.

This paper proposes a zonal-based optimal microgrid identification model that boosts identifying the microgrid's optimal topology in current distribution systems. The model accordingly identifies the optimal location and size of the DERs that are installed within the defined area of the centralized microgrid. Consequently, the proposed model can effectively reduce the complexity that arises from installing DERs by centralizing their installations in a specific area (i.e., within the optimal topology of the microgrid) instead of randomly distributing them over the distribution network. Moreover, the proposed study can efficiently accelerate realizing the envisioned smart grids due to considering current distribution networks to incorporate the installation of the microgrids, which in turn facilitate the integration of DERs, including renewable energy resources and battery energy storage systems (BESS). The main contributions of this paper are summarized as follows:

- A zonal-based microgrid identification model was developed to identify the optimal zone topology that is defined based on the optimal centralized microgrid physical boundaries;
- The model was developed as a mixed-integer linear programming (MILP) problem that effectively reduces the computational time and significantly decreases the complexity in solving the power flow optimization problem;
- The proposed optimization approach is capable of determining the optimal sizes and locations of the DERs that would be installed in the centralized microgrids. Moreover, the impact of incorporating the BESS was considered and analyzed.

The rest of the paper is structured as follows: Section 2 discusses the model outline of the proposed zonal-based optimal microgrids identification, Section 3 introduces the problem formulation of the proposed model, Section 4 presents numerical simulations on a distribution network test system, and Section 5 concludes the paper and highlights the key points.

2. Model Outline

The proposed model recognizes the centralized microgrid physical boundaries (i.e., buses numbers that can be grouped to form a microgrid within existing distribution systems) by utilizing a linearized power flow model. This centralized microgrid can effectively mitigate the need to upgrade current distribution systems, facilitate controlling the microgrid operation, and enhance the entire system reliability by increasing the DERs installations. This model optimally identifies the largest feasible DERs that can be installed within the determined zone.

Figure 1 demonstrates the flowchart of the proposed model. The model calculates the optimal linear power flow to ensure the system's feasibility. It should be mentioned that the applied AC linear power flow model overcomes the issues associated with the high R/X ratio, unlike the classical power flow analysis techniques such as Newton Raphson and Gauss–Seidel methods, which are not suitable for radial distribution systems [51–53]. Therefore, the linearization of the AC power flow equation provides the required information in the power flow analysis of radial distribution systems with a high level of accuracy in voltage magnitude and angle values. The optimal linear power flow is subject to the distribution system operational constraints, which include active and reactive power flow limits and voltage variation limits. In addition, it is capable of identifying the optimal regional zone within the distribution network to be a centralized microgrid based on developed constraints that take into account line lengths and buses correlation. It should be mentioned that the DERs surplus generation beyond local loads demand (i.e., loads demand within the identified microgrid) is computed to be utilized to supply other buses loads of the

distribution system. The impact of installing additional BESS on the system is considered by involving the BESS constraints, which is predicted to increase the DERs installation.
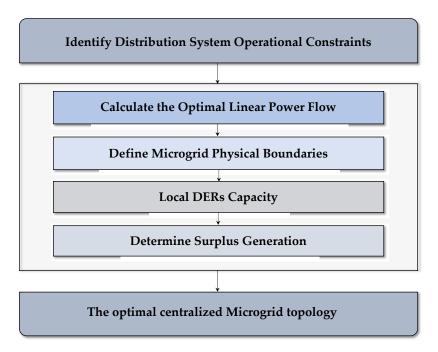

Figure 1. Flowchart of the proposed model.

3. Problem Formulation

This section proposes the mathematical problem formulation that allocates centralized microgrids into existing distribution systems while maximizing DERs installations.

3.1. Objective Function

The objective function in Equation (1) of the proposed model is to maximize the DERs installations in the selected centralized microgrid topology.

$$\max \sum_{m \in Z} P_m^{DER} \tag{1}$$

This objective is subject to the following equality and inequality constraints that are described in the following subsections. Moreover, maximizing the DERs into the selected zone represents the maximum available amount of power that can be distributed within the microgrid.

3.2. Microgrid Topology Constraints

The centralized microgrid topology is defined based on the declared line distances between buses, the connectivity of distribution buses, and the radiality structure of the entire distribution system. The zone area of the centralized microgrid is mathematically defined as follows:

$$\lambda_{mn}^{\min} \leq Z \qquad \forall mn \in L \tag{2}$$

$$Z \leq \sum_{n \in L_m} \lambda_{mn} U_{mn} \qquad \forall m \in B \tag{3}$$

Equation (2) ensures that each created zone is equal to or larger than the minimum declared distance, which is the least line lengths between the distribution system's buses. Therefore, this constraint drives the model to create the largest feasible zones topologies that are used to determine the microgrid physical boundaries. Equation (3) is presented to determine that each zone size is designed based on the total lines' lengths. However, it further excludes any bus that is connected with more than two buses from the zone area.

This can be achieved by the existence of the binary variable *U*, which is equal to zero if the selected bus is connected with more than two buses, and one otherwise. In other words, this binary variable is used to guarantee that each bus within the microgrid topology must not be connected to more than two lines. Equations (2) and (3) act together to ensure that the microgrid can be designed without impacting the operation of the entire distribution system.

It should be mentioned that the connectivity of all buses is guaranteed based on the power flow active and reactive constraints, which is demonstrated in the following subsection.

3.3. Linear Power Flow Constraints

Linear power flow models overcome the main challenges and drawbacks of nonlinear models. The AC power flow linearization algorithm proposed in [16] is used in this model as follows:

$$\sum_{c \in G} P_c^M + \sum_{n \in L_m} PL_{mn} + P_m^{DER} + P_m^B = P_m^D \qquad \forall m \in B \tag{4}$$

$$\sum_{c \in G} Q_c^M + \sum_{n \in L_m} QL_{mn} + Q_m^{DER} = Q_m^D \qquad \forall m \in B \tag{5}$$

$$-P_c^{M,\max} \le P_c^M \le P_c^{M,\max} \qquad \forall c \in G \tag{6}$$

$$-Q_c^{M,\max} \le Q_c^M \le Q_c^{M,\max} \qquad \forall c \in G \tag{7}$$

$$PL_{mn} = g_{mn}\left(1 + \Delta\hat{V}_m\right)(\Delta V_m - \Delta V_n) - b_{mn}(\Delta\theta_m - \Delta\theta_n) \qquad \forall mn \in L \tag{8}$$

$$QL_{mn} = -b_{mn}\left(1 + \Delta\hat{V}_m\right)(\Delta V_m - \Delta V_n) - g_{mn}(\Delta\theta_m - \Delta\theta_n) \qquad \forall mn \in L \tag{9}$$

$$-PL_{mn}^{\max} \le PL_{mn} \le PL_{mn}^{\max} \qquad \forall mn \in L \tag{10}$$

$$-QL_{mn}^{\max} \le QL_{mn} \le QL_{mn}^{\max} \qquad \forall mn \in L \tag{11}$$

$$\Delta V_m^{\min} \le \Delta V_m \le \Delta V_m^{\max} \qquad \forall m \in B \tag{12}$$

The objective of maximizing the installed DERs in the centralized microgrid is subject to the equality and inequality Equations (4)–(12). The active and reactive power balance Equations (4) and (5) are used in this model to ensure that the total generated power supplies the total distribution loads. In these active and reactive power balance equations, the total generated power is defined as the total power supplied from the upstream grid and the available power that can be supplied by the installed DERs. The total power supplied from the upstream grid will be defined based on the upper and lower bounds Equations (6) and (7) for the active and reactive supplied power, respectively. The active and reactive power flow between two adjacent buses is defined based on the linear power flow Equations (8) and (9), respectively. In Equations (8) and (9), voltage values in all buses are defined based on their deviation from the voltage magnitude of the upstream grid, i.e., $\Delta V_m = 1 - V_m$. The value of $\Delta\hat{V}_m$ is defined as a constant value that represents the calculated deviation in bus *m*, which is calculated in a previous step in the linearization process. Moreover, g_{mn} and b_{mn} represent the conductance and susceptance of the line between buses *m* and *n*, respectively. The active and reactive power flow equations are limited by their upper and lower bounds in Equations (10) and (11), respectively. Equation (12) represents the minimum and maximum voltage variation limits for all buses. In the designed model, the active and reactive power balance equations are used to guarantee the connectivity of the centralized microgrid within the entire distribution system.

3.4. Battery Energy Storage System

The installation of the BESS in the microgrid is subject to the following constraints:

$$P^{R,\min} \le P_m^R \le P^{R,\max} \qquad \forall m \in B \tag{13}$$

$$E^{R,\min} \leq E_m^R \leq E^{R,\max} \qquad \forall m \in B \tag{14}$$

$$0 \leq P_m^{dch} \leq P^R v_m \qquad \forall m \in B \tag{15}$$

$$-P^R u_m \leq P_m^{ch} \leq 0 \qquad \forall m \in B \tag{16}$$

$$P_m^B = P_m^{dch} + P_m^{ch} \qquad \forall m \in B \tag{17}$$

$$E_m^B = \boldsymbol{H}_m^B - \frac{P_m^{dch}}{\eta} - P_m^{ch} \qquad \forall m \in B \tag{18}$$

$$u_m + v_m \leq 1 \qquad \forall m \in B \tag{19}$$

Rated power and energy limits of BESS are constrained in Equations (13) and (14), respectively. The maximum and minimum charging and discharging power are constrained in Equations (15) and (16), respectively. It is worth mentioning that the BESS power is perceived as positive during discharging mode as it is producing power, whilst it is considered negative during charging mode as it is consuming power in this condition. Equation (17) indicates the BESS output power as it involves the summation of BESS discharging and charging power. The BESS available hourly stored energy is calculated based on the available energy at the past hour minus the discharged/charged power while considering the energy storage efficiency in Equation (18). Consequently, the BESS available stored energy increases when it is charged and decreases when it is discharged. Binary variables u and v specify the charging and discharging states, respectively. Therefore, Equation (19) confirms that the BESS operates in only one operation mode at each time period, i.e., either in charging or discharging mode.

4. Numerical Simulations

In this paper, the IEEE 33-bus distribution test system was utilized to examine the performance and robustness of the proposed model. The tested system consists of 33 load buses and 32 lines, as shown in Figure 2. The line and bus data are provided in detail in [54]. The main feeder, which is set at bus 1, connects the entire distribution system with the upstream grid, while the system is tested on the baseload values 3.715 MW and 2.3 MVar. Based on the proposed model, the connectivity of the entire distribution system with the upstream grid would not be impacted by the defined centralized microgrid. Nonetheless, the defined microgrid can be isolated from the entire distribution system through the point of the common coupling (PCC). The PCC is the point that electrically connects the centralized microgrid to the entire distribution system. In addition, it is worth mentioning that, in the centralized microgrid, the minimum rated power of the installed DERs is zero, while the maximum rated power of DERs is the maximum available installed capacity. The problem is formulated as a mixed-integer linear programming (MILP) problem in the General Algebraic Modeling System (GAMS) platform and solved using CPLEX 11.0 [55]. The following three cases are studied:

Case 1: Optimal centralized microgrid topology including optimal DERs capacity;
Case 2: The impact of installing BESS to the optimal centralized microgrid topology;
Case 3: Comparison between the proposed method and other optimization methods.

The objective of Case 1 is to demonstrate the optimal centralized microgrid topology based on the proposed approach. The largest possible centralized zones that could be deployed as microgrids are investigated in this case. In addition, the optimal zone is determined based on its capability to supply total load, i.e., the load within its geographical boundaries, while accommodating the largest capacity of DERs. By performing this approach, the negative impact of allocating DERs "randomly" throughout the entire distribution system is mitigated due to installing DERs into only selected optimal centralized microgrid.

On the other hand, the purpose of performing Case 2 is to illustrate the impact of installing BESS on identifying the optimal centralized zone. In this case, the BESS is used to enhance the penetration of renewable energy resources and increase the DERs installation. It should be indicated that the optimal BESS capacity should be defined based on available

charging and discharging capacities. Furthermore, Case 3 is provided to compare the proposed method with other existing methods in the literature.
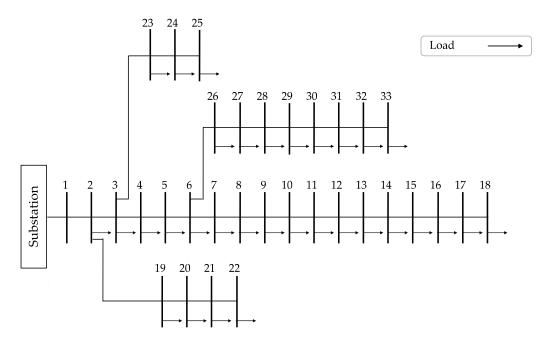

Figure 2. IEEE-33 bus distribution test system.

Case 1: The optimal centralized microgrid topology is defined based on the considered operational constraints. The obtained largest four possible centralized microgrids are demonstrated in detail in Table 1 and shown in Figure 3. This table provides the acquired zones configurations that include buses numbers, lines numbers, PCC locations, and the aggregated total lines distance. The obtained four centralized zones are: (i) Zone A: includes buses 7 through 18, lines 7 through 17, and coupled to the other parts of distribution grid at the PCC at line 6; (ii) Zone B: includes buses 19 through 22, lines 19 through 21, and coupled to the other parts of distribution grid at the PCC at line 18; (iii) Zone C: includes buses 23 through 25, lines 23 and 24, and coupled to the other parts of distribution grid at the PCC at line 22; and (iv) Zone D: includes buses 26 through 33, lines 26 and 32, and coupled to the other parts of distribution grid at the PCC at line 25.

Table 1. Zones Topology.

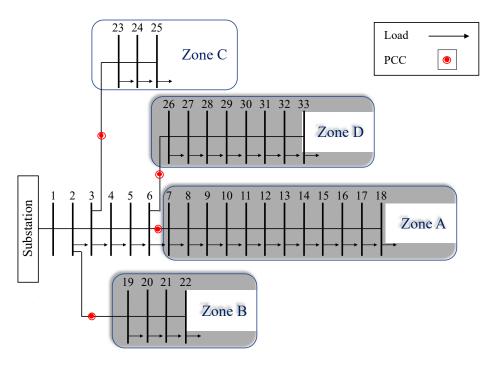| Zone	Quantity	Zone Configurations
Zone A	Bus #	7, 8, 9, 10, 11, 12, 13, 14, 15, 16, 17, 18
	Line #	7, 8, 9, 10, 11, 12, 13, 14, 15, 16, 17
	PCC	Line 6
	Total Distance (m)	8650
Zone B	Bus #	19, 20, 21, 22
	Line #	19, 20, 21
	PCC	Line 18
	Total Distance (m)	2600
Zone C	Bus #	23, 24, 25
	Line #	23, 24
	PCC	Line 22
	Total Distance (m)	1800
Zone D	Bus #	26, 27, 28, 29, 30, 31, 32, 33
	Line #	26, 27, 28, 29, 30, 31 32
	PCC	Line 25
	Total Distance (m)	4200

#. The number sign.

Figure 3. IEEE-33 bus distribution system, including largest possible centralized zones.

Based on the optimal results, each generated centralized zone has specific characteristics, which are illustrated in Table 2. As demonstrated in this table, the optimal centralized zone to be selected as a centralized microgrid is Zone A. In Zone A, the total installed DERs capacity reaches 2590.40 kW, while the total served load is 1075 kW, which implies that this system has a surplus generation of 1515.40 kW that can be used to supply other parts of the distribution grid. On the other side, Zone B accommodates the lowest DERs capacity with only 860.90 kW while supplying a total load of 360 kW; thus, Zone B has only 500.90 kW surplus generation. The remaining two zones, i.e., Zone C and Zone D, provide 1983.02 kW DERs installation capacity, 930 kW total served load, and 1053.02 kW surplus generation and 2442.16 kW DERs installation capacity, 920 kW total served load, and 1522.16 kW surplus generation, respectively.

Table 2. Optimal Operational Results in Case 1.

Zone	Quantity	Operational Results
Zone A	DERs Capacity (kW)	2590.40
	Total Distance (m)	8650
	Total Load (kW)	1075
	Percentage of Served Load (%)	100
	Surplus Generation (kW)	1515.40
Zone B	DERs Capacity (kW)	860.90
	Total Distance (m)	2600
	Total Load (kW)	360
	Percentage of Served Load (%)	100
	Surplus Generation (kW)	500.90
Zone C	DERs Capacity (kW)	1983.02
	Total Distance (m)	1800
	Total Load (kW)	930
	Percentage of Served Load (%)	100
	Surplus Generation (kW)	1053.02
Zone D	DERs Capacity (kW)	2442.16
	Total Distance (m)	4200
	Total Load (kW)	920
	Percentage of Served Load (%)	100
	Surplus Generation (kW)	1522.16

When comparing Zone A with the other three zones, Zone A: accommodates DERs capacity of 200.89% more than Zone B, 30.63% more than Zone C, and 6.07% more than Zone D; supplies a total load of 198.61% more than Zone B, 15.59% more than Zone C, and 16.85% more than Zone D; has surplus generation of 202.53% more than Zone B, 43.91% more than Zone C, and 0.45% less than Zone D.

Even though Zone D has a higher surplus generation compared with Zone A, Zone A is selected to be the optimal centralized microgrid over Zone D as it accommodates a larger amount of DERs installation, which is considered to be the first criteria for identifying the optimal centralized zone. Accordingly, this case study validates the effectiveness of the proposed model to identify not only the optimal centralized microgrid configuration but also the optimal DERs location and capacity as well as the capability of enhancing the surplus generation of the entire distribution system.

Case 2: In this case study, the same IEEE-33 bus distribution test system is used; however, the objective here is to investigate the impact of installing additional BESS on the optimal results of identifying the centralized microgrid. BESS is used to support the utilization of renewable energy resources by storing surplus generation of dispatchable and non-dispatchable units and maximizing the overall DERs installation of the system. The maximum stored energy is defined based on the maximum available BESS capacity to be accommodated by the centralized microgrid. It should be mentioned that the BESS efficiency and the stored energy at the preceding hour are assumed to be 95% and 0, respectively. The impact of installing BESS on the centralized microgrids is demonstrated in Table 3. The optimal results indicate that the BESS capacity is 400 kW at 7, 135 kW at bus 19, 110 kW at bus 23, and 520 kW at bus 26 for Zones A, B, C, and D, respectively. The total generation and surplus generation of the four centralized microgrids are shown in Figure 4. The obtained four centralized zones provide the following values: Zone A accommodates a total DERs of 2990.41 kW with 64.05% surplus generation; Zone B accommodates a total DERs of 995.91 kW with 63.85% surplus generation; Zone C accommodates a total DERs of 2093.02 kW with 55.56% surplus generation; Zone D accommodates a total DERs of 2962.16 kW with 68.94% surplus generation.

Table 3. Optimal Operational Results in Case 2.

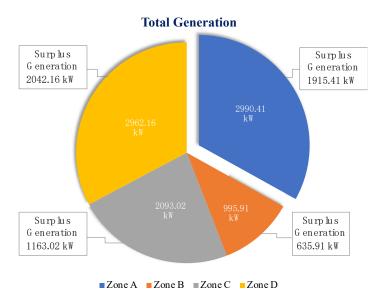| Zone	Quantity	Operational Results
Zone A	DERs Capacity (kW)	2990.41
	Total Distance (m)	8650
	Total Load (kW)	1075
	Percentage of Served Load (%)	15.44
	Surplus Generation (kW)	1915.41
Zone B	DERs Capacity (kW)	995.91
	Total Distance (m)	2600
	Total Load (kW)	360
	Percentage of Served Load (%)	15.68
	Surplus Generation (kW)	635.91
Zone C	DERs Capacity (kW)	2093.02
	Total Distance (m)	1800
	Total Load (kW)	930
	Percentage of Served Load (%)	5.54
	Surplus Generation (kW)	1163.02
Zone D	DERs Capacity (kW)	2962.16
	Total Distance (m)	4200
	Total Load (kW)	920
	Percentage of Served Load (%)	21.29
	Surplus Generation (kW)	2042.16

Total Generation

Figure 4. Optimal DERs capacity for Case 2, including surplus generation.

Figure 5 shows the percentage of the BESS capacity out of the total DERs in each centralized zone. Based on the optimal results, Zone A is also determined as the optimal centralized microgrid in the system, which accommodates the largest DERs capacity. On the other hand, it is worth indicating that Zone D has the heights surplus generation compared with the other three zones; however, based on the proposed model, this elevation of surplus generation does not impact the determination of the optimal centralized zone, as it is considered as a secondary standard when the optimal results deliver symmetrical values.
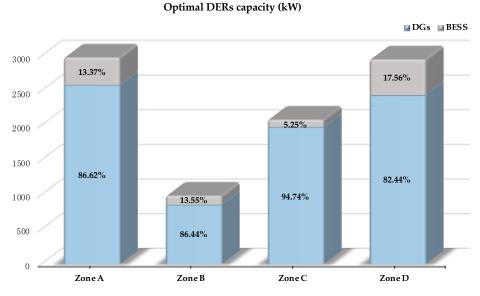
Optimal DERs capacity (kW)

Figure 5. Total DERs capacity demonstrating the percentage of BESS installation.

When comparing the obtained results in this case with Case 1, the optimal DERs capacity increased by 15.44%, 15.68%, 5.54%, and 21.29% for Zones A, B, C, and D, respectively. Consequently, this case demonstrates the significant impact of installing BESS on increasing the DERs installation along with enhancing surplus generation availability on the overall distribution system. In other words, the optimal results of these case studies indicate that the proposed approach can efficiently mitigate the need to upgrade existing distribution systems by maximizing the DERs installation. Nonetheless, a larger distribution system can be utilized without loss of generality.

Case 3: In this case, the simulation results of the proposed method are compared with other optimization methods presented in [53–57]. The objective of these methods is to maximize the amount of DERs installed in distribution systems. In addition, it is worth mentioning that all compared studies utilize the same IEEE-33 bus test system with the same base load values of 3.715 + j 2.3 MVA. Table 4 compares and summarizes the obtained results of the proposed optimization method with the other techniques, including Stud Krill herd Algorithm (SKHA) [53], Particle Swarm Optimization algorithm (PSO) [56], and Gravitational search algorithm (GSA) [57].

Table 4. Comparison Between the Proposed Method and Other Methods.

Method	Zone Topology	Number of Iterations	Computational Time	Optimal DERs Capacity	Optimal Locations
Particle Swarm Optimization Algorithm (PSO) [56]	Zone 4 (buses 6–11, and 26)	250 iterations	not stated	1175 kW	bus 8
Stud Krill herd Algorithm (SKHA) [53]	Entire distribution system	100 iterations	4.2406 s	2590 kW	bus 6
Gravitational Search Algorithm (GSA) [57]	Zone 3 (buses 9–18)	solved in two phases with many iterations (not stated)	not stated	2589 kW	bus 6
Proposed Method (Case 1)	Zone A (buses 7–18)	1 iteration	1.1321 s	2590 kW	bus 7
Proposed Method (Case 2)	Zone A (buses 7–18)	1 iteration	1.1327 s	2990 kW	bus 7

The superiority of the proposed approach is highlighted in Table 4. Although the obtained results in Case 1 provide an almost similar amount of DERs installation compared to the results of the other optimization methods (increased by: 120.5%, and 0.034% compared to [56,57], respectively), it delivers diverse locations of the installed DERs with a different microgrid topology. On the other hand, the compression between the obtained results of Case 2 with the other optimization methods indicates an obvious increase in the DERs penetration (increased by: 154.5%, 15.4%, and 15.5% compared to [53,56,57], respectively). Accordingly, the obtained results of the proposed method (Case 2) provide the optimal centralized microgrid topology with its optimal installed DERs, i.e., 2990 kW. Furthermore, it is worth mentioning that the proposed method is a linearized method, which reduces the complexity in solving the power flow optimization problem (i.e., it does not require several iterations compared to the other techniques) and significantly reduces the computational time to 1.1321 sec, and 1.1327 sec, for Cases 1 and 2, respectively. Consequently, it can be summarized that the obtained results demonstrate the merits and effectiveness of the proposed method over the other optimization methods reported in the literature.

5. Conclusions

This paper developed a zonal-based optimal microgrid identification model, which utilized a power flow linearization technique to find the optimal solution. How to identify the optimal location and size of a centralized microgrid within existing distribution systems was researched and investigated in this paper, accompanied by maximizing distributed generators installations to support the operation of distribution grids. Integrating a centralized microgrid within current distribution grids could postpone the need to upgrade systems and expedite incorporating such techniques in a modernized manner. Numerical simulations on the IEEE-33 bus test distribution system illustrated the merits and effectiveness of the proposed model on identifying the optimal centralized microgrid zonal area

and its significance on maximizing the installation of distributed energy resources to be hosted in the microgrid.

Nomenclature

Indices:

c	Index for point of interconnection
ch	Superscript for energy storage charging mode
dch	Superscript for energy storage discharging mode
m,n	Index for buses
$\wedge$	Index for calculated variables

Sets:

B	Set of buses
G	Set of points connected to upstream grid
L	Set of distribution lines
Lm	Set of distribution lines connected to bus m
Z	Set of zones

Parameters:

b	Susceptance of the line between connected buses
$E^{R,max}$	Maximum rated energy of BESS
$E^{R,min}$	Minimum rated energy of BESS
g	Conductance of the line between connected buses
P^D	Load active power
$P^{M,max}$	Maximum active power exchange with upstream grid
$P^{R,max}$	Maximum rated power of BESS
$P^{R,min}$	Minimum rated power of BESS
PL^{max}	Maximum active power flow between connected buses
Q^D	Load reactive power
$Q^{M,max}$	Maximum reactive power exchange with upstream grid
QL^{max}	Maximum reactive power flow between connected buses
ΔV^{max}	Maximum deviation in bus voltage magnitude
ΔV^{min}	Minimum deviation in bus voltage magnitude
H^B	Stored energy at preceding hour
λ	Line length between connected buses
λ^{min}	Minimum line length between connected buses
η	BESS efficiency

Variables:

E^B	Stored energy of BESS
E^R	Rated energy of BESS
P^B	Output power of BESS
P^{ch}	Charged power of BESS
P^{dch}	Discharged power of BESS
P^{DER}	Distributed energy resources active power
P^M	Active power exchange with upstream grid
P^R	Rated power of BESS
PL	Active power flow between connected buses
Q^{DER}	Distributed energy resources reactive power
Q^M	Reactive power exchange with upstream grid
QL	Reactive power flow between connected buses
U	Distribution bus connection state
ΔV	Deviation in bus voltage magnitude
$\Delta \theta$	Deviation in voltage angle
u	BESS discharging state
v	BESS charging state

References

1. Vakulchuk, R.; Overland, I.; Scholten, D. Renewable energy and geopolitics: A review. *Renew. Sustain. Energy Rev.* **2020**, *122*, 109547. [CrossRef]
2. Ajeigbe, O.A.; Munda, J.L.; Hamam, Y. Optimal allocation of renewable energy hybrid distributed generations for small-signal stability enhancement. *Energies* **2019**, *12*, 4777. [CrossRef]
3. Alturki, M.; Khodaei, A. Marginal hosting capacity calculation for electric vehicle integration in active distribution networks. In Proceedings of the 2018 IEEE/PES Transmission and Distribution Conference and Exposition (T&D), Denver, CO, USA, 16–19 April 2018; pp. 1–9. [CrossRef]
4. Elavarasan, R.M.; Shafiullah, G.M.; Padmanaban, S.; Kumar, N.M.; Annam, A.; Vetrichelvan, A.M.; Mihet-Popa, L.; Holm-Nielsen, J.B. A comprehensive review on renewable energy development, challenges, and policies of leading indian states with an international perspective. *IEEE Access* **2020**, *8*, 74432–74457. [CrossRef]
5. Şerban, A.C.; Lytras, M.D. Artificial intelligence for smart renewable energy sector in Europe—Smart energy infrastructures for next generation smart cities. *IEEE Access* **2020**, *8*, 77364–77377. [CrossRef]
6. Turner, J.A. A realizable renewable energy future. *Science* **1999**, *285*, 687–689. [CrossRef]
7. Abbassi, R.; Abbassi, A.; Jemli, M.; Chebbi, S. Identification of unknown parameters of solar cell models: A comprehensive overview of available approaches. *Renew. Sustain. Energy Rev.* **2018**, *90*, 453–474. [CrossRef]
8. Pravitasari, D.; Nisworo, S. New and renewable energy: A review and perspectives. In Proceedings of the 2017 IEEE International Conference on Sustainable Information Engineering and Technology (SIET), Malang, Indonesia, 24–25 November 2017; pp. 284–287.
9. Pali, B.S.; Vadhera, S. Renewable energy systems for generating electric power: A review. In Proceedings of the 2016 IEEE 1st International Conference on Power Electronics, Intelligent Control and Energy Systems (ICPEICES), Delhi, India, 4–6 July 2016; pp. 1–6.
10. Alturki, M.; Khodaei, A. Increasing distribution grid hosting capacity through optimal network reconfiguration. In Proceedings of the 2018 IEEE North American Power Symposium (NAPS), Fargo, ND, USA, 9–11 September 2018; pp. 1–6. [CrossRef]
11. Puri, V.; Jha, S.; Kumar, R.; Priyadarshini, I.; Son, L.H.; Abdel-Basset, M.; Elhoseny, M.; Long, H.V. A hybrid artificial intelligence and internet of things model for generation of renewable resource of energy. *IEEE Access* **2019**, *7*, 111181–111191. [CrossRef]
12. Marcos, F.P.; Domingo, C.M.; Román, T.G.S.; Arín, R.C. Location and sizing of micro-grids to improve continuity of supply in radial distribution networks. *Energies* **2020**, *13*, 3495. [CrossRef]
13. Shahidehpour, M.; Clair, J.F. A functional microgrid for enhancing reliability, sustainability, and energy efficiency. *Electr. J.* **2012**, *25*, 21–28. [CrossRef]
14. Albaker, A.; Khodaei, A. Elevating prosumers to provisional microgrids. In Proceedings of the 2017 IEEE Power & Energy Society General Meeting, Chicago, IL, USA, 16–20 July 2017; pp. 1–5.
15. Justo, J.J.; Mwasilu, F.; Lee, J.; Jung, J.-W. AC-microgrids versus DC-microgrids with distributed energy resources: A review. *Renew. Sustain. Energy Rev.* **2013**, *24*, 387–405. [CrossRef]
16. Alturki, M.; Khodaei, A.; Paaso, A.; Bahramirad, S. Optimization-based distribution grid hosting capacity calculations. *Appl. Energy* **2018**, *219*, 350–360. [CrossRef]
17. Office of Electricity Delivery and Energy Reliability. DOE Microgrid Workshop Report. Summary Report 2012. Available online: https://www.energy.gov/sites/prod/files/Microgrid%20Workshop%20Report%20August%202011.pdf (accessed on 24 September 2021).
18. Takano, H.; Goto, R.; Hayashi, R.; Asano, H. Optimization method for operation schedule of microgrids considering uncertainty in available data. *Energies* **2021**, *14*, 2487. [CrossRef]

19. Albaker, A.; Khodaei, A. Valuation of microgrid unused capacity in islanded operation. In Proceedings of the 2017 North American Power Symposium (NAPS), Morgantown, WV, USA, 17–19 September 2017; pp. 1–6.

20. Asano, H.; Hatziargyriou, N.; Iravani, R.; Marnay, C. Microgrids: An overview of ongoing research, development, and demonstration projects. *IEEE Power Energy Mag.* **2007**, *5*, 78–94.

21. Albaker, A.; Khodaei, A. Optimal scheduling of integrated microgrids in holonic distribution grids. In Proceedings of the 2018 IEEE North American Power Symposium (NAPS), Fargo, ND, USA, 9–11 September 2018; pp. 1–6. [CrossRef]

22. Khodaei, A. Provisional microgrids. *IEEE Trans. Smart Grid* **2014**, *6*, 1107–1115. [CrossRef]

23. Ghalavand, F.; Alizade, B.A.M.; Gaber, H.; Karimipour, H. Microgrid islanding detection based on mathematical morphology. *Energies* **2018**, *11*, 2696. [CrossRef]

24. Kroposki, B.; Lasseter, R.; Ise, T.; Morozumi, S.; Papathanassiou, S.; Hatziargyriou, N. Making microgrids work. *IEEE Power Energy Mag.* **2008**, *6*, 40–53. [CrossRef]

25. Shahidehpour, M. Role of smart microgrid in a perfect power system. In Proceedings of the 2010 IEEE PES General Meeting, Minneapolis, MN, USA, 25–29 July 2010; p. 1.

26. Khodaei, A. Microgrid optimal scheduling with multi-period islanding constraints. *IEEE Trans. Power Syst.* **2013**, *29*, 1383–1392. [CrossRef]

27. Talapur, G.G.; Suryawanshi, H.M.; Xu, L.; Shitole, A.B. A reliable microgrid with seamless transition between grid connected and islanded mode for residential community with enhanced power quality. *IEEE Trans. Ind. Appl.* **2018**, *54*, 5246–5255. [CrossRef]

28. Albaker, A.; Majzoobi, A.; Zhao, G.; Zhang, J.; Khodaei, A. Privacy-preserving optimal scheduling of integrated microgrids. *Electr. Power Syst. Res.* **2018**, *163*, 164–173. [CrossRef]

29. Parhizi, S.; Lotfi, H.; Khodaei, A.; Bahramirad, S. State of the art in research on microgrids: A review. *IEEE Access* **2015**, *3*, 890–925. [CrossRef]

30. Alam, M.N.; Chakrabarti, S.; Ghosh, A. Networked microgrids: State-of-the-art and future perspectives. *IEEE Trans. Ind. Inform.* **2018**, *15*, 1238–1250. [CrossRef]

31. Hossain, E.; Kabalci, E.; Bayindir, R.; Perez, R. Microgrid testbeds around the world: State of art. *Energy Convers. Manag.* **2014**, *86*, 132–153. [CrossRef]

32. Cagnano, A.; De Tuglie, E.; Mancarella, P. Microgrids: Overview and guidelines for practical implementations and operation. *Appl. Energy* **2020**, *258*, 114039. [CrossRef]

33. Hasanvand, S.; Nayeripour, M.; Waffenschmidt, E.; Fallahzadeh-Abarghouei, H. A new approach to transform an existing distribution network into a set of micro-grids for enhancing reliability and sustainability. *Appl. Soft Comput.* **2017**, *52*, 120–134. [CrossRef]

34. Di Fazio, A.R.; Russo, M.; De Santis, M. Zoning evaluation for voltage optimization in distribution networks with distributed energy resources. *Energies* **2019**, *12*, 390. [CrossRef]

35. Osama, R.A.; Zobaa, A.F.; Abdelaziz, A.Y. A planning framework for optimal partitioning of distribution networks into microgrids. *IEEE Syst. J.* **2019**, *14*, 916–926. [CrossRef]

36. Wang, G.; Wang, Q.; Qiao, Z.; Wang, J.; Anderson, S. Optimal planning of multi-micro grids based-on networks reliability. *Energy Rep.* **2020**, *6*, 1233–1249. [CrossRef]

37. Tsikalakis, A.G.; Hatziargyriou, N.D. Centralized control for optimizing microgrids operation. *IEEE Trans. Energy Convers.* **2008**, *1*, 241–248. [CrossRef]

38. Mojtahedzadeh, S.; Najafi-Ravadanegh, S.; Haghifam, M.R. A framework for optimal clustering of a greenfield distribution network area into multiple autonomous microgrids. *J. Power Technol.* **2016**, *96*, 219–228.

39. Oh, Y.S.; Cho, G.J.; Kim, M.S.; Kim, J.S.; Bukhari, S.B.; Haider, R.; Zaman, M.S.; Kim, C.H. Zonal operation scheme of distributed generations for voltage regulation in distribution networks. In Proceedings of the International Conference on Power Systems Transients (IPST2017), Seoul, Korea, 26–29 June 2017; pp. 26–29.

40. Li, P.; Liu, J.; Li, B.; Song, Y.; Zhong, J. Dynamic power system zone division scheme using sensitivity analysis. *J. Int. Counc. Electr. Eng.* **2014**, *4*, 157–161. [CrossRef]

41. Pachanapan, P.; Anaya-Lara, O.; Dysko, A.; Lo, K.L. Adaptive zone identification for voltage level control in distribution networks with DG. *IEEE Trans. Smart Grid* **2012**, *3*, 1594–1602. [CrossRef]

42. Meng, T.; Xu, M.; Zou, G.; Yang, J.; Zhang, J.; Lin, X. Voltage regulation based on hierarchical and district-dividing control for active distribution network. In Proceedings of the 2015 IEEE PES Asia-Pacific Power and Energy Engineering Conference (APPEEC), Brisbane, QLD, Australia, 15–18 November 2015; pp. 1–5. [CrossRef]

43. Lotfi, H.; Ghazi, R.; Naghibi-Sistani, M.B. Multi-objective dynamic distribution feeder reconfiguration along with capacitor allocation using a new hybrid evolutionary algorithm. *Energy Syst.* **2020**, *11*, 779–809. [CrossRef]

44. Lotfi, H.; Ghazi, R. Optimal participation of demand response aggregators in reconfigurable distribution system considering photovoltaic and storage units. *J. Ambient Intell. Humaniz. Comput.* **2021**, *12*, 2233–2255. [CrossRef]

45. Lotfi, H. Multi-objective energy management approach in distribution grid integrated with energy storage units considering the demand response program. *Int. J. Energy Res.* **2020**, *44*, 10662–10681. [CrossRef]

46. Di Fazio, A.R.; Russo, M.; de Santis, M. Zoning evaluation for voltage vontrol in smart distribution networks. In Proceedings of the IEEE International Conference on Environment and Electrical Engineering (EEEIC), Palermo, Italy, 12–15 June 2018.

47. Kiran, D.; Abhyankar, A.R.; Panigrahi, B.K. Hierarchical clustering based zone formation in power networks. In Proceedings of the 2016 National Power Systems Conference (NPSC), Bhubaneswar, India, 19–21 December 2016; pp. 1–6.

48. Pandit, M.; Srivastava, L.; Sharma, M.; Dubey, H.M.; Panigrahi, B.K. Large-scale multi-zone optimal power dispatch using hybrid hierarchical evolution technique. *J. Eng.* **2014**, *2014*, 71–80. [CrossRef]

49. Islam, S.R.; Sutanto, D.; Muttaqi, K. Coordinated decentralized emergency voltage and reactive power control to prevent long-term voltage instability in a power system. *IEEE Trans. Power Syst.* **2014**, *30*, 2591–2603. [CrossRef]

50. Cotilla-Sanchez, E.; Hines, P.D.; Barrows, C.; Blumsack, S.; Patel, M. Multi-attribute partitioning of power networks based on electrical distance. *IEEE Trans. Power Syst.* **2013**, *28*, 4979–4987. [CrossRef]

51. Yuan, H.; Li, F.; Wei, Y.; Zhu, J. Novel linearized power flow and linearized OPF models for active distribution networks with application in distribution LMP. *IEEE Trans. Smart Grid* **2016**, *9*, 438–448. [CrossRef]

52. Nikmehr, N.; Ravadanegh, S.N. Heuristic probabilistic power flow algorithm for microgrids operation and planning. *IET Gener. Transm. Distrib.* **2015**, *9*, 985–995. [CrossRef]

53. ChithraDevi, S.; Lakshminarasimman, L.; Balamurugan, R. Stud krill herd algorithm for multiple DG placement and sizing in a radial distribution system. *Eng. Sci. Technol. Int. J.* **2017**, *20*, 748–759. [CrossRef]

54. Ghasemi, S.; Moshtagh, J. Radial distribution systems reconfiguration considering power losses cost and damage cost due to power supply interruption of consumers. *Int. J. Electr. Eng. Inform.* **2013**, *5*, 297–315. [CrossRef]

55. ILOG CPLEX Homepage. 2009. Available online: http://www.ilog.com (accessed on 21 May 2021).

56. Mohamed, A.A.R.; El-Sharkawy, R.; Omran, W.A. Power management strategy to enhance the operation of active distribution networks. In Proceedings of the IEEE 2017 5th International Istanbul Smart Grid and Cities Congress and Fair (ICSG), Istanbul, Turkey, 19–21 April 2017; pp. 95–99.

57. Murty, V.V.V.S.N.; Kumar, A. Optimal DG integration and network reconfiguration in microgrid system with realistic time varying load model using hybrid optimisation. *IET Smart Grid* **2019**, *2*, 192–202. [CrossRef]